Hindawi
Journal of Chemistry
Volume 2022, Article ID 5375815, 14 pages
https://doi.org/10.1155/2022/5375815

Research Article

Aspartic Acid- and Glycine-Functionalized Mesoporous Silica as an Effective Adsorbent to Remove Methylene Blue from Contaminated Water

Abdullah M. Alswieleh

Department of Chemistry, College of Science, King Saud University, Riyadh, Saudi Arabia

Correspondence should be addressed to Abdullah M. Alswieleh; aswieleh@ksu.edu.sa

Received 26 February 2022; Revised 6 April 2022; Accepted 12 April 2022; Published 26 April 2022

Academic Editor: Ahmed Mourtada Elseman

In this work, aspartic acid- and glycine-functionalized mesoporous silica nanoparticles (Asp-MSNs and Gly-MSNs) were successfully prepared and applied as adsorbents for removal of methylene blue (MB) from contaminated water. The mesoporous structure of the fabricated nanomaterials was confirmed by nitrogen adsorption/desorption with specific surface area of ca. 700 m^2/g and pore volume of 0.9 cm^3/g for both Asp-MSNs and Gly-MSNs. The average size of the nanoadsorbents was estimated to be ca. 290 nm as characterized by scanning electron microscopy (SEM) and transmission electron microscope (TEM). The physical and chemical properties of the Asp-MSNs and Gly-MSNs were also characterized by Fourier transform infrared (FTIR) spectroscopy, zeta potential, and elemental analysis. Asp-MSNs and Gly-MSNs exhibited good adsorption performance for removal of cationic organic dyes (MB). The equilibrium adsorption capacity of Asp-MSNs and Gly-MSNs was found to be 55 $mg{\cdot}g^{-1}$ and 43 $mg{\cdot}g^{-1}$, respectively, under the optimal conditions. The Langmuir model and pseudo-second-order equation exhibited good correlation with the isotherm and adsorption kinetic data for MB, respectively.

1. Introduction

Water pollution with organic dyes from industries, such as leather, plastic, cosmetics, paper, food, and textile, has been a serious environmental issue. Wastewater contaminated with such compounds may create an eco-toxic hazard and cause bioaccumulation. Thus, the decontamination of wastewater has received a great deal of attention worldwide. [1] Most of the organic dyes are very stable and difficult to be biodegraded. [2] Exposure to such hazardous dyes may cause neurological injury, nausea, and vomiting. Due to the strong toxicity in plants, animals, and humans, hazardous dyes should be removed from wastewater before discharging to the environment. [3, 4]

Several physical, chemical, and biological treatment techniques have been developed to decontaminate wastewater. [3–6] Among these techniques, adsorption method has proven to be simple, effective, and economically feasible method for treating of dye-containing wastewater. [6–8] Therefore, different types of adsorbents have been developed to meet different needs, such as activated carbon [9], clay [10], and zeolite. [11] However, such adsorbents have some limitations such as low adsorption capacities and regeneration problems. [4, 6] Therefore, new adsorbents with high adsorption performance are needed to develop.

In recent years, nanostructured materials have been widely explored as high-efficiency sorbents due to their high surface area and high activities. [12–14] Mesoporous silica nanoparticles (MSNs) have been widely researched in biological and environmental fields, because of the excellent structural features, thermal stability, facile modification, and high surface area. [15–17] MSNs have been modified with different functional groups to increase the extraction efficiency, such as amine [18–22] or carboxylic acid [23, 24]. Amine-functionalized MSNs have been fabricated as an adsorbent to remove alizarin yellow and phenol red from wastewater with maximum adsorption capacity of 370.70 $mg\,g^{-1}$ and 400 $mg\,g^{-1}$, respectively. [21] Moreover,

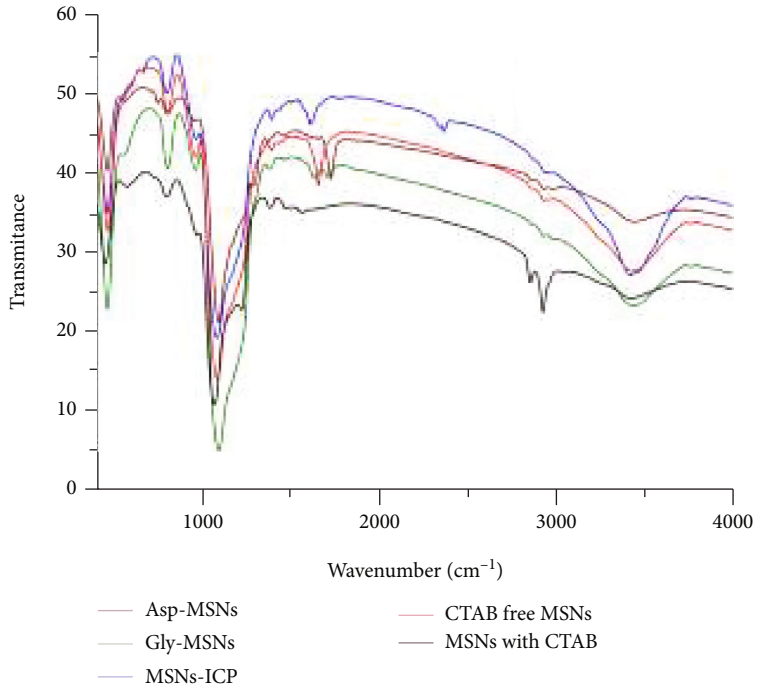

Figure 1: FTIR spectra of (black) MSNs (with CTAB), (red) CTAB free MSNs, (blue) MSNs-ICP, (brown) Asp-MSNs, and (green) Gly-MSNs.

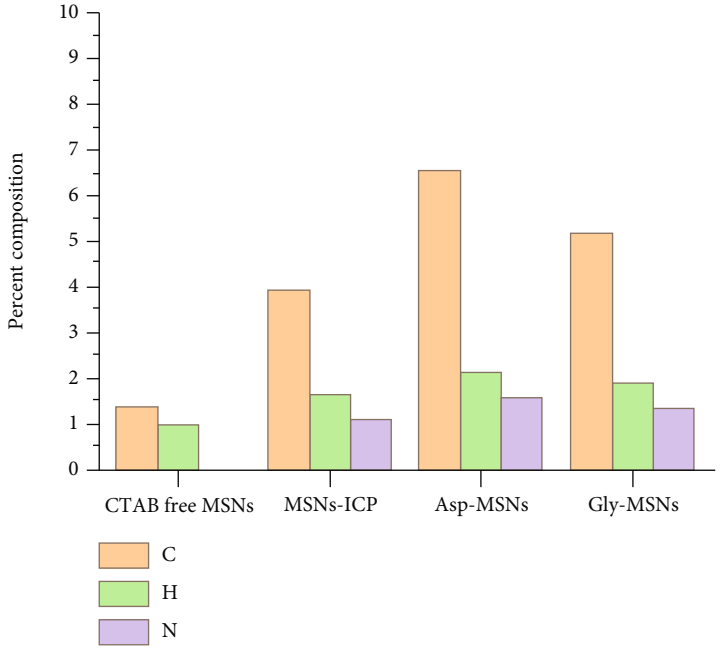

Figure 2: Elemental analysis for CTAB free MSNs, MSNs-ICP, Asp-MSNs, and Gly-MSNs.

amine-modified porous silica was used to remove Ponceau 4R, Rhodamine B, Sunset Yellow, and Brilliant Blue from aqueous solutions with more than 92% extraction efficiency. [22] MSNs modified with carboxylic acid have also been used as adsorbent for removal phenosafranine (PF), methylene blue (MB), rhodamine B (RhB), and orange II (OII), with high extraction capacities for cationic dyes. [23]

Amine and carboxylic groups on the surface may improve the adsorption of ionic organic molecules. The attachment of amino acids on the surface of the adsorbents improved the adsorption efficiency of organic molecules. [25–29] Beagan reported the synthesis of MSNs via Stober method and functionalized with cysteine for removal MB from contaminated water using the batch method. [27]

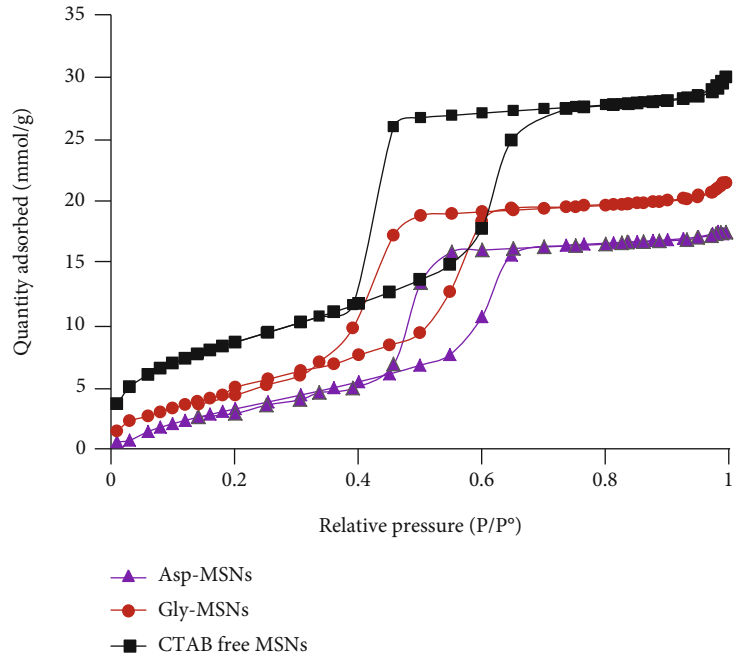

Figure 3: The isotherm obtained for CTAB free MSNs, Gly-MSNs, and Asp-MSNs.

The adsorption capacity was about 70 mg/g in acidic media, and about 140 mg/g in basic media. Histidine attached to MSNs surface was synthesized to remove MB from an aqueous solution. [28] The maximum adsorption efficiency of the fabricated nanoparticles was reported to be 60 mg/g in basic media.

As far as I am aware, very little work has been reported on MSNs modification with amino acids for environmental applications. Hence, in this study, mesoporous silica nanoparticles (MSNs) were combined with amino acids to prepare novel nanosorbents (Asp-MSNs and Gly-MSNs) for the removal of cationic dye (methylene blue (MB)). Therefore, anchoring of aspartic acid and glycine onto the MSNs surface is beneficial for improving the adsorption capacities of MB. The fabricated Asp-MSNs and Gly-MSNs were characterized by FTIR, zeta potential, SEM, and TEM analyses. Batch adsorption tests of MB by Asp-MSNs and Gly-MSNs were carried out at different pH values, initial concentration, and contact time, to study the adsorption kinetics and isotherms.

2. Experimental

2.1. Materials. N-Cetyltrimethylammonium bromide (CTAB, 98%), n-hexane (99%), ammonium hydroxide (NH_4OH, 32 wt%), tetraethyl orthosilicate (TEOS, 98%), dichloromethane (DCM, HPLC grade), 3-isocyanatopropyl triethoxysilane (ICPTES, >95%), L-aspartic acid (Asp, ≥98%), and glycine (Gly, ≥98.5%) were obtained from Sigma-Aldrich. Toluene (98%), hydrochloric acid (HCl, 36%), sodium hydroxide, dimethylformamide (DMF, HPLC grade), pyridine (analytical grade), methanol (HPLC grade), and ethanol (HPLC grade) were brought from Fisher Scientific. Methylene blue (MB) was brought from WINLAB. All chemicals were used as received.

Table 1: Comparison of the surface area, pore volume, and pore size of CTAB free MSNs, Gly-MSNs, and Asp-MSNs.

	Surface area (m^2/g)	Pore volume (cm^3/g)	Pore size (nm)
CTAB free MSNs	1019	1.37	5.5
Gly-MSNs	739	0.92	4.9
Asp-MSNs	684	0.87	4.7

2.2. Fabrication of the Nanoadsorbents

2.2.1. Synthesis of Mesoporous Silica Nanoparticles (MSNs). 160 mL of distilled water (DW), CTAB (1 g), and NH_4OH (4 mL) were added and stirred at 40°C. A mixture of TEOS and n-hexane (25 mL) with 4 : 1 ratio was added slowly to the aqueous solution. The solid was separated and washed with DW and methanol several times. Then, the particles were suspended in 25 mL of acetic acid (12.5 mL) and hydrogen peroxide (12.5 mL) at 120°C. Finally, the solid was separated and washed with DW and methanol several times [30–32].

2.2.2. Aspartic Acid- and Glycine-Functionalized MSNs. The synthesis of aspartic acid-functionalized MSNs (Asp-MSNs) and glycine-functionalized MSNs (Gly-MSNs) was achieved in two steps. Firstly, 1 g of CTAB free MSNs was dispersed in 25 mL dried toluene and sonicated for 10 min. ICPTES (0.2 mL) was added to the mixture and heated at 120°C overnight. MSNs-ICP was separated and washed with dry toluene and DMF. Secondly, MSNs-ICP was suspended in 10 mL DMF and sonicated for 10 min.

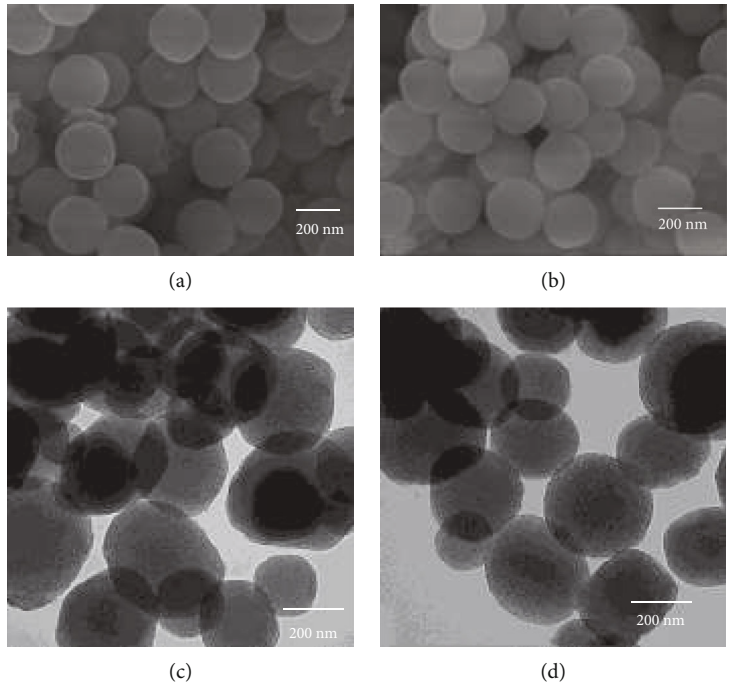

Figure 4: (a) and (b) SEM images of Asp-MSNs and Gly-MSNs, respectively. (c) and (d) TEM images of Asp-MSNs and Gly-MSNs, respectively.

To the suspension, 10 mL of DMF containing 200 mg of aspartic acid (or glycine) was added and sonicated for 10 min. The mixture was left under stirring at room temperature overnight. Asp-MSNs (or Gly-MSNs) were separated and washed with DW and methanol several times, and dried at 90°C for 3 h.

2.3. General Characterization. The structure and performance of the fabricated nanoadsorbents were characterized using several techniques. Scanning electron microscopy (SEM) images were obtained using JEOL instrument model JSM-6380 LA. Transmission electron microscopy (TEM) images were obtained using JEOL instrument model JEM-1230. The FTIR spectra measurements were mounted using Thermo Scientific Nicolet iS10 FT-IR spectrometer in KBr pellet at room temperature in a spectral range 4000–400 cm^{-1}. Shimadzu instrument model UV-2600 was used to acquire UV spectra of dye.

2.4. Adsorption Investigation

2.4.1. Batch Adsorption Experiments. Batch method experiments were performed using MB as probes to evaluate the adsorption performance of fabricated nanoadsorbents. The adsorption behavior was investigated at different pH values, initial concentration, and exposure time. The contaminated water samples were prepared by dissolving known amounts of MB in DW. The prepared adsorbent (10 mg) was placed in a sample tube containing 10 mL of different concentrations MB aqueous solution (20, 50, 80, 100, 200 mg·L) and then shaken at 150 r·min^{-1} for certain period time. The nanoadsorbents were separated by centrifugation and the concentration of MB after adsorption process was determined by UV–vis spectrophotometer. The removal efficiency and the amount of MB adsorbed onto nanoadsorbents were calculated using the following equations:

$$\begin{aligned} \text{Removal efficiency}(\%) &= C_0 - C_e/C_0 \times 100\%, \\ q_t &= (C_0 - C_t)V/m, \end{aligned} \tag{1}$$

where C_0 and C_e (mg·L) are the initial and equilibrium concentrations of MB, respectively. C_t (mg·L) is the concentration of MB at time t (min). q_t (mg·g^{-1}) is the amount of MB adsorbed per unit mass of the nanoadsorbents at time t. V (L) is the volume of the adsorbed solution. m (g) is the mass of the nanoadsorbents.

2.4.2. Adsorption Kinetics. The kinetics of MB adsorbed on the surface of the nanoadsorbents was explained by three adsorption models. Each equation model is expressed by:

(i) Pseudo-first-order model

$$l_g(q_e - q_t) = l_g q_e - k_1 t, \tag{2}$$

(ii) Pseudo-second-order model

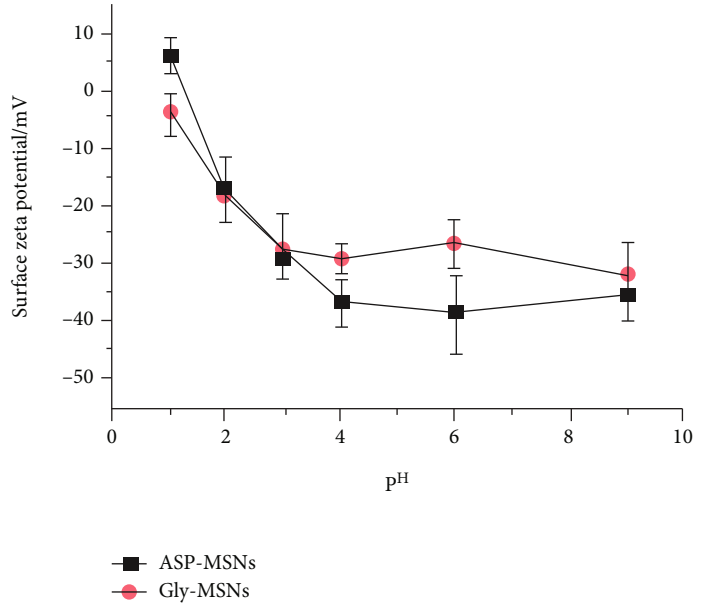

Figure 5: The electronic charges on the surface of Asp-MSNs and Gly-MSNs in aqueous solutions at different pH values.

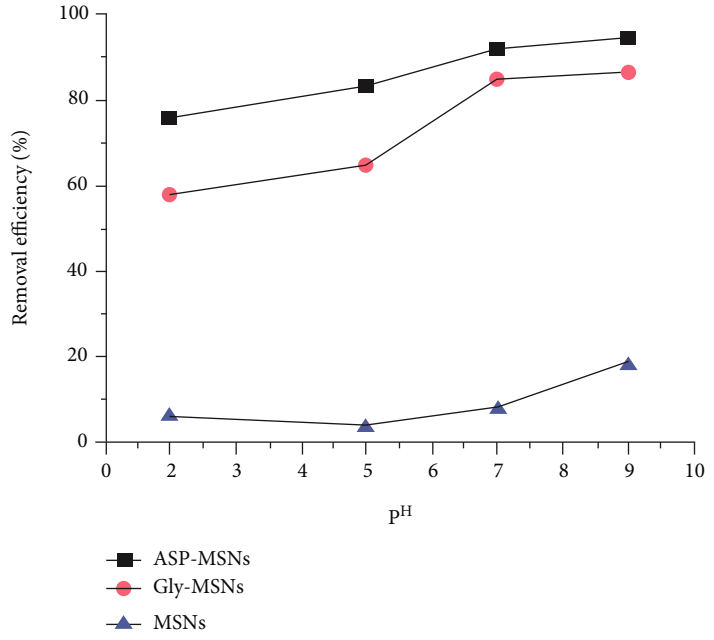

Figure 6: Effect of pH on adsorption behavior of MB by CTAB free MSNs, Asp-MSNs, and Gly-MSNs (C_0 = 50 mg·L, V =10 mL, T =298 K).

$$\frac{t}{q_t} = \frac{1}{k_2 q_e^2} + \frac{t}{q_e}, \tag{3}$$

(iii) Intraparticle diffusion model

$$q_t = k_{\text{dif}} t^{1/2} + C, \tag{4}$$

where q_e (mg·g^{-1}) is the amount of MB adsorbed onto the nanoadsorbents at equilibrium. q_t (mg·g^{-1}) is the amount of MB adsorbed onto the nanoadsorbents at time t (min). k_1 (mg·min·g^{-1}) is the pseudo-first-order rate constant. k_2 (mg·min·g^{-1}) is the pseudo-second-order rate constant. $k_2 q_e^2$ is the initial sorption rate (mg·g^{-1}·min^{-1}), revealing the movement rate of MB molecule. k_{dif} (mg·g^{-1}·min$^{-1/2}$) is the intraparticle diffusion rate constant.

2.4.3. Adsorption Isotherms. To understand the adsorption behavior of MB on the surface of nanoadsorbents, two isotherm equations were selected to model the adsorption

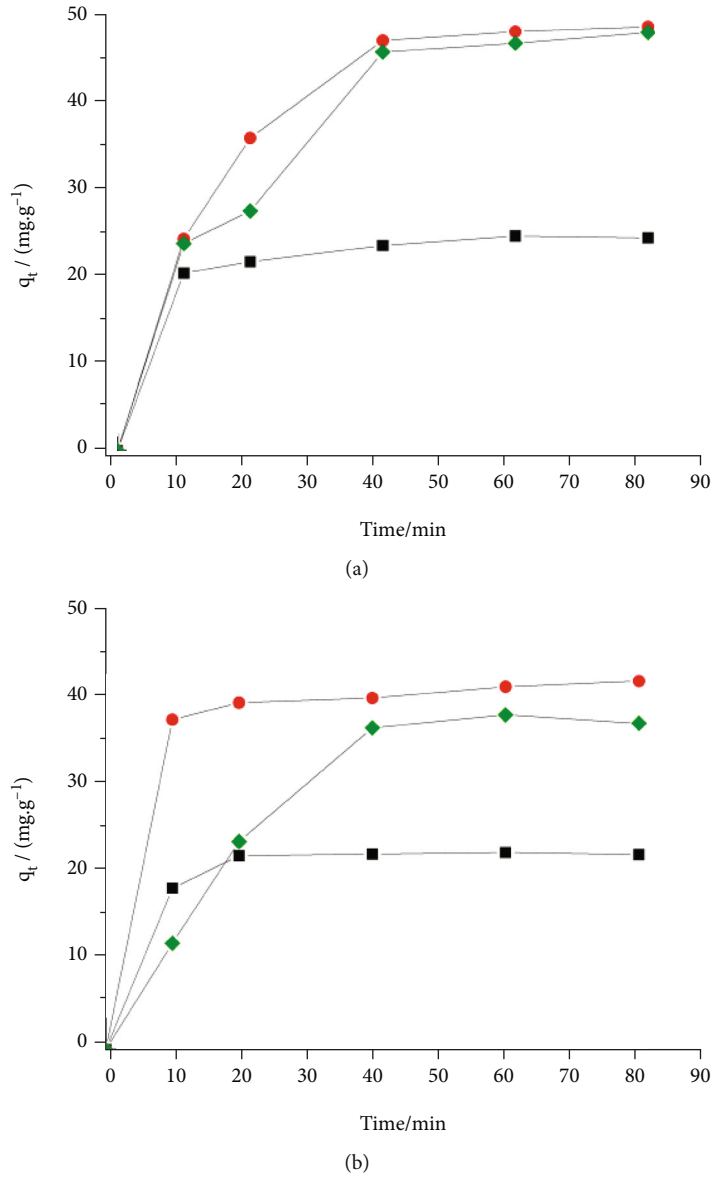

Figure 7: Effect of contact time and initial concentration (50 ppm (black), 100 ppm (green), and 200 ppm (red)) on adsorption behavior of MB by (a) Asp-MSNs and (b) Gly-MSNs (V =10 mL, T =298 K).

isotherm data. The Langmuir and Freundlich equation models are expressed by:

Langmuir equation:

$$\frac{C_e}{q_e} = \frac{1}{bq_m}\frac{C_e}{q_m}, \tag{5}$$

Freundlich equation:

$$\ln q_e = \ln K_f + \frac{1}{n} \ln C_e, \tag{6}$$

where q_m (mg·g^{-1}) is the maximum adsorption capacity. K_F is the constant related to the adsorption intensity. b (L·mg^{-1}) is the Langmuir constant which is related to the affinity of the binding site. A smaller value of $(1/n)$ suggests a more heterogeneous surface. However, when the value is equal or closer to one suggests that the adsorbent has relatively more homogeneous binding sites.

3. Results and Discussion

3.1. General Characterization. Asp-MSNs (or Gly-MSNs) were fabricated in four steps. In basic solution and presence of template (CTAB) and expander agent (hexane), condensation reaction of TEOS was carried out to obtain MSNs. CTAB was extracted by ion exchange process using a mixture of acetic acid and hydrogen peroxide, to have hydrophilic surface and allow reaction with inner surface. CTAB free MSNs were reacted with ICPTES through hydrolysis and condensation reactions between the silanol groups of MSNs and alkoxysilane groups of ICPTES to obtain isocyanato groups conveniently attached to MSNs surface. The primary amine groups in aspartic acid and glycine could

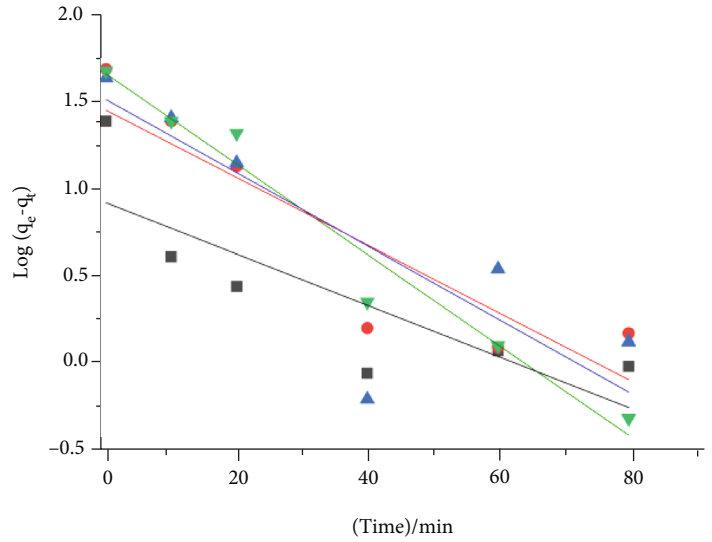

(a)

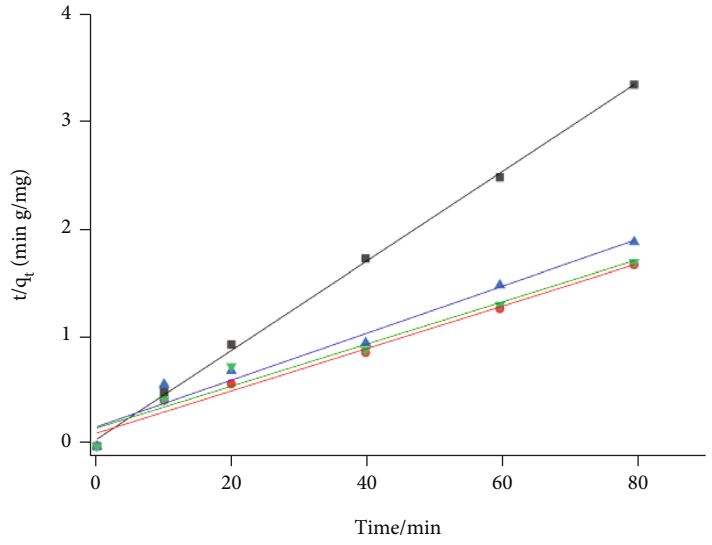

(b)

Figure 8: Continued.

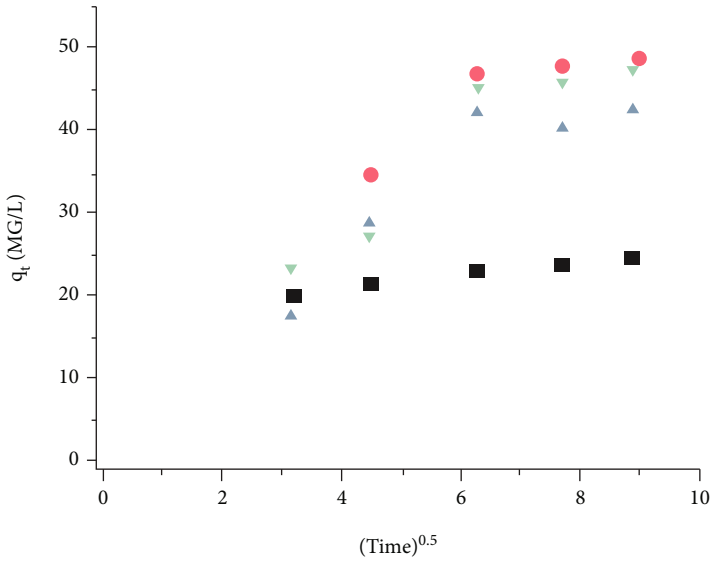

(c)

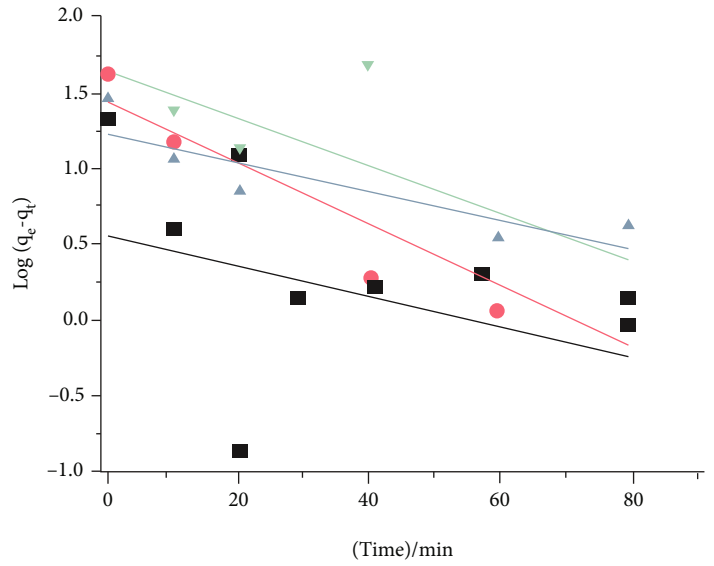

(d)

Figure 8: Continued.

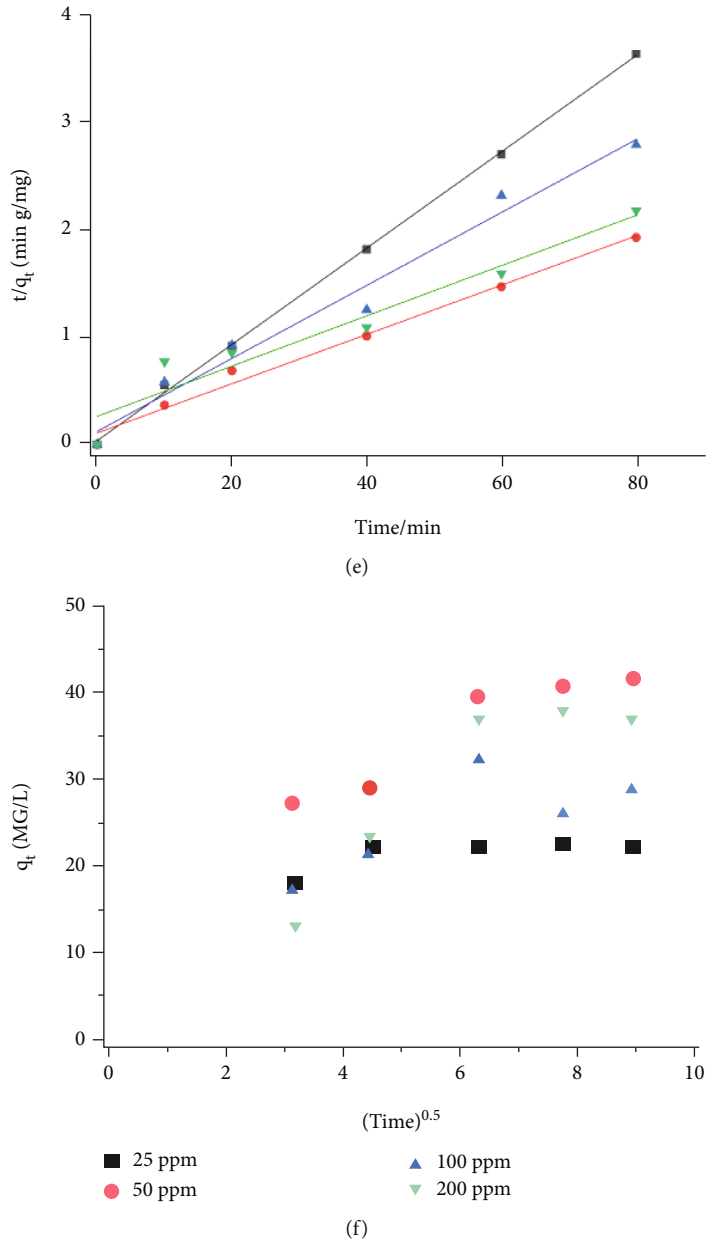

Figure 8: (a) Pseudo-first-order kinetics, (b) pseudo-second-order kinetics, and (c) intraparticle diffusion kinetics for adsorption of MB on Asp-MSNs. (d) Pseudo-first-order kinetics, (e) pseudo-second-order kinetics, and (f) intraparticle diffusion kinetics for adsorption of MB on Gly-MSNs (m =10 mg, V =10 mL, pH =7, and T =298 K).

react with isocyanato groups on the surface, producing Asp-MSNs (or Gly-MSNs).

The covalent functionalization of MSNs with aspartic acid and glycine was characterized by FTIR spectroscopy. Figure 1 shows the IR spectra for MSNs (with CTAB), CTAB free MSNs, MSNs-ICP, Asp-MSNs, and Gly-MSNs. Peaks at ~450 cm^{-1} (SiO_4, tetrahedron vibration) and ~800cm^{-1} (Si –O–Si, symmetric vibration) were noted. Peaks were observed between 1300 and 1000 cm^{-1}, ascribed to Si–O bands stretching of the silica network. A large band at 3400 cm^{-1} was observed for SiO–H. [33] Two bands located at ~2920 cm^{-1} and 2855 cm^{-1} due to $-CH_2-$ stretching vibrations of CTAB in MSNs (with CTAB) sample, which disappeared after solvent extraction process of CTAB, indicating the successful removal of the template from the pores of MSNs. [28, 29] In the MSNs-ICP spectrum, the peak appearing at ~2900 cm^{-1} and~1440 cm^{-1} corresponded to the C–H groups. In the Asp-MSNs and Gly-MSNs spectra, peak located at ~1720 cm^{-1} was observed, corresponding to the carbonyl (–CO–) presence in aspartic acid and glycine, which indicated the successful grafting of amino acids onto the MSNs surface.

In order to confirm the presence of aspartic acid and glycine components in Asp-MSNs and Gly-MSNs, elemental analysis was used to estimate the percentages of carbon, hydrogen, and nitrogen in CTAB free MSNs, MSNs-ICP,

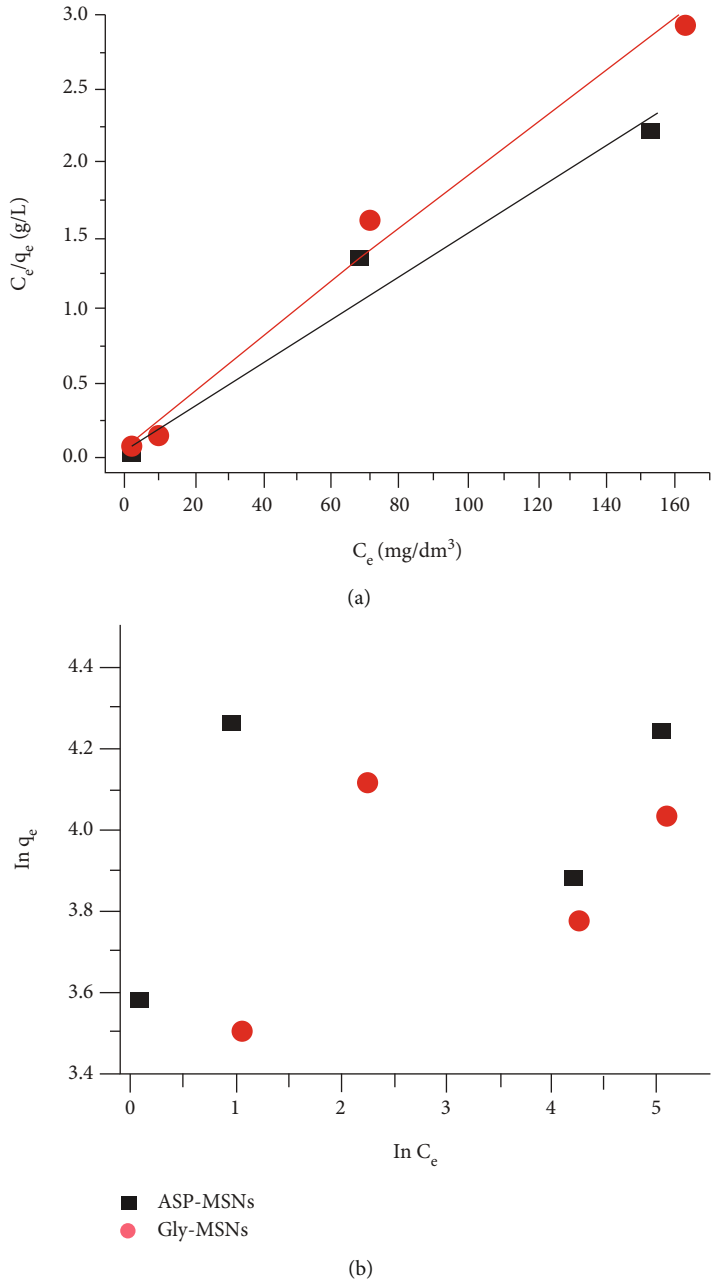

Figure 9: (a) Langmuir adsorption isotherm fit of MB onto Asp-MSNs and Gly-MSNs, and (b) Freundlich adsorption isotherm fit of MB onto Asp-MSNs and Gly-MSNs (m =10 mg, V =10 mL, pH =7, and T =298 K).

Asp-MSNs, and Gly-MSNs. As seen from Figure 2, there is an increase in amount of the C, H, and N elements at each step in the surface modification, which indicated the successful attachment of aspartic acid and glycine onto MSNs surfaces.

The texture properties of CTAB free MSNs, Gly-MSNs, and Asp-MSNs were studied by the N_2 adsorption-desorption isotherm. The BET surface area, total pore volume, and pore sizes were analyzed using Micromeritics Gemini 2375 instrument. It was observed that all the analyzed samples exhibited type IV isotherm with H_1 hysteresis loop, which is typical for mesoporous materials, as shown in Figure 3. This isotherm suggested the adsorption process on the surface of fabricated nanoparticles via multilayer adsorption followed by capillary condensation. Small different capillary condensation steps were found for modified nanoparticles (Gly-MSNs and Asp-MSNs) at higher relative pressures, compared with CTAB free MSNs. The presence of functional groups on MSNs surface reduced its effective silanol surface area. Moreover, the CTAB free MSNs pore diameter was smaller after surface modification due to the presence of functional groups on the internal and external pore surface, leading to the reduction in pore volume; the data are summarized in Table 1.

The SEM and TEM images were utilized to study the morphology of Asp-MSNs and Gly-MSNs. Representative images illustrated in Figures 4(a)–4(d) clearly showed that both Asp-MSNs and Gly-MSNs were almost spherical in shape particles with an average particles size of 290 nm. In addition, TEM images revealed that MSNs have well-ordered pores with an average pore size of 6 nm, which agreed with BET pore size.

The electronic charges on the surface of Asp-MSNs and Gly-MSNs in aqueous solutions at different pH values can be analyzed by zeta potentials. As shown in Figure 5, the result indicated that when the pH was higher than 2 (at pH above the pK_a of carboxylic acid), the surface charge of both nanoadsorbents was negatively charged due to the deprotonation of the carboxylic acid groups. Asp-MSNs and Gly-MSNs are expected to exhibit increased adsorption capacities at pH above the pK_a of carboxylic acid groups, since the electrostatic interactions usually dominate the adsorption process of cationic dyes.

3.2. Effect of pH on the Removal Efficiency. It has been reported that pH is an important parameter affecting the adsorption of organic dyes from contaminated water; [34, 35] therefore, a series of batch equilibrium experiments were conducted to study the effect of pH on the adsorption efficiency of MB by nanoadsorbents over a range of pH values. Figure 6 shows the removal efficiency of MB by CTAB free MSNs, Asp-MSNs, and Gly-MSNs as a function of the corresponding solution pH. According to the surface zeta potential obtained by DLS, as the pH of the solution increased, the surface zeta potential of Asp-MSNs and Gly-MSNs became more negative. Consequently, the adsorption capacities of adsorbents increased due to the electrostatic attractions between the surface of the nanoadsorbents and MB. When the pH of 50 ppm MB solution reached 9, the removal efficiency of MB by Asp-MSNs and Gly-MSNs was 95% and 87%, respectively, compared to 17% for CTAB free MSNs.

3.3. Effect of Contact Time and Initial Concentration on the Removal Efficiency. The contact time is an important parameter for evaluating the adsorption properties of nanoadsorbents. Figures 7(a) and 7(b) show the influence of the contact time and initial concentration on the adsorption capacities of MB by Asp-MSNs and Gly-MSNs. At all concentrations, the removal efficiency increased sharply within 10 min and reached equilibrium in 90 min. The adsorption sites on Asp-MSNs and Gly-MSNs for the MB were sufficient in the initial stage of the adsorption process. When the contact time increases, sufficient interactions can occur between the dye and the adsorption sites of nanoadsorbents. As time progressed, the number of adsorption sites was occupied by MB, and the adsorption capacities were eventually saturated. MB molecules have good mobility and reached equilibrium in a short time due to their low molecular weight and planar structure. [36]

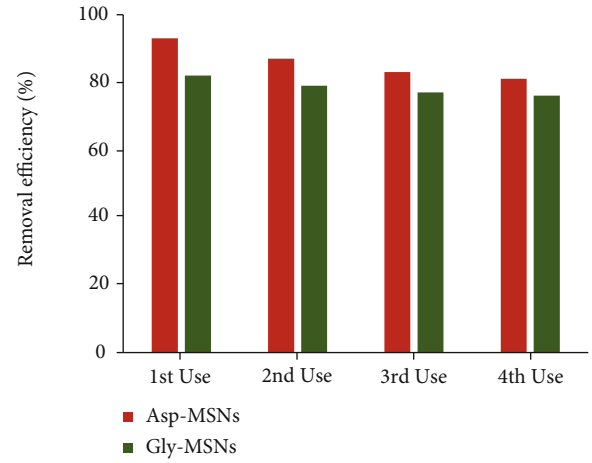

Figure 10: Adsorption efficiency of the fresh Asp-MSNs and Gly-MSNs (1st use) and that of the regenerated nanoadsorbents after two, three, and four uses in the removal of MB from contaminated water at $C_0 = 50$ mg·L, $V = 10$ mL, $T = 298$ K, and pH = 7.

3.4. Adsorption Kinetics. The kinetics of the MB adsorbed onto Asp-MSNs and Gly-MSNs were described by adsorption (equations (2), (3), and (4)). Figures 8(a)–8(c) show the linear fitting results of the kinetic data. The obtained experimental data fitted better with the pseudo-second-order kinetic model (MB on Asp-MSNs: $R^2 = 0.962$, MB on Gly-MSNs: $R^2 = 0.948$). These results suggested that the adsorption rate of MB on the nanoadsorbents was primarily controlled by chemisorption. Since there are electron-rich functional groups on the surface of the nanoadsorbent, then these groups provide attraction forces with dye. Furthermore, the calculated q_e from the pseudo-second order was 52.63 mg·g^{-1} for MB on Asp-MSNs, and 42.92 mg·g^{-1} for MB on Gly-MSNs, which were close to the experimental data (49.7 mg·g^{-1} for MB on Asp-MSNs, and 41.8 mg·g^{-1} for MB on Gly-MSNs).

3.5. Adsorption Isotherms. Two isotherm models, Langmuir and Freundlich, were selected to fit the adsorption isotherm data, to understand the adsorption behavior of nanoadsorbents. The fitted results of the selected isotherm models are presented in Figure 9. According to the correlation coefficients (R^2), the Langmuir model was found to be more suitable than the Freundlich model for describing the adsorption of MB onto Asp-MSNs and Gly-MSNs with correlation coefficients of 0.949 and 0.961, respectively. These results suggested that the surface of both Asp-MSNs and Gly-MSNs were coated by a monolayer of the dye. The maximum adsorption capacity of MB calculated from the Langmuir model was found to be 68.58 mg·g^{-1} and 55.11 mg·g^{-1} for Asp-MSNs and Gly-MSNs, respectively.

3.6. Nanoadsorbents Reusability. The spent nanoadsorbents after use under the optimal set of conditions ($C_0 = 50$ mg·L,

Table 2: The maximum adsorption capacities of different adsorbents for removing MB from aqueous solution, reported in the past literatures.

Adsorbents	q_e (mg·g^{-1})	Ref
Amine functionalized mesoporous silica	49	[37]
Mesoporous silica with cyclodextrin	60	[38]
Histidine modified mesoporous silica	60	[28]
Mesoporous silica functionalized with carboxylic groups	43	[39]
Mesoporous silica coated chitosan	43	[40]
Cysteine functionalized mesoporous silica	140	[27]
Aspartic acid-functionalized MSNs (Asp-MSNs)	55	In this study
Glycine-functionalized MSNs (Gly-MSNs)	43	In this study

V =10 mL, T =298 K, and pH =7) were then washed with acidic solution and ethanol, and then reused under the same optimal conditions. The adsorption efficiencies obtained with successive reuse of the nanoadsorbents are shown in Figure 10. The adsorption efficiencies obtained after two, three, and four uses of Gly-MSNs 1.05-, 1.1-, and 1.13-fold lower than that for the unused Gly-MSNs, whereas the adsorption efficiencies obtained after two, three, and four uses of Asp-MSNs 1.04-, 1.06- and 1.1-fold lower than that for the unused Asp-MSNs.

To illustrate the adsorption performance of Asp-MSNs and Gly-MSNs, the maximum adsorption capacities of nanoadsorbents for MB were compared with those of other reported adsorbents. In general, the maximum adsorption capacities of the fabricated nanoadsorbents for MB were close to most of the other adsorbents, as reported in Table 2. Considering the convenient synthetic method and good adsorption performance, Asp-MSNs and Gly-MSNs are good absorbents for removing toxic cationic molecules from polluted water.

4. Conclusion

In this study, a simple and effective approach based on surface modification of mesoporous silica nanoparticles (MSNs) with amino acids was developed to obtain nanoadsorbents with good adsorption performances. Both Asp-MSNs and Gly-MSNs exhibited good removal properties of MB from aqueous solutions. The equilibrium adsorption capacity of Asp-MSNs was 55 mg·g^{-1}, whereas the equilibrium adsorption capacity of Gly-MSNs was 43 mg·g^{-1}, at 298 K. The experimental data from the adsorption kinetics and isotherm studies indicated that the adsorption of pollutant on both nanoadsorbents fitted well with the pseudo-second-order equation and Langmuir model, respectively. Based on the high efficiency and feasibility, Asp-MSNs and Gly-MSNs exhibited good potential for water treatment.

Data Availability

The data presented in this study are included in this article.

Conflicts of Interest

The authors declare no conflict of interest.

Acknowledgments

This project was supported by Researchers Supporting Project number RSP-2021/238, King Saud University, Riyadh, Saudi Arabia.

References

[1] K. Miksch, G. Cema, P. F.-X. Corvini et al., "R&D priorities in the field of sustainable remediation and purification of agro-industrial and municipal wastewater," *New Biotechnology*, vol. 32, no. 1, pp. 128–132, 2015.

[2] H. Zollinger, Ed., *Azo Dyes and Pigments, Colour Chemistry-Synthesis*, Properties and Applications of Organic Dyes and Pigments, New York, 1987.

[3] E. Forgacs, T. Cserháti, and G. Oros, "Removal of synthetic dyes from wastewaters: a review," *Environment International*, vol. 30, no. 7, pp. 953–971, 2004.

[4] A. Sintakindi and B. Ankamwar, "Fungal biosorption as an alternative for the treatment of dyes in waste waters: a review," *Environmental Technology Reviews*, vol. 10, no. 1, pp. 26–43, 2021.

[5] T. Ilame and A. Ghosh, "The Promising Applications of Nanoparticles for Synthetic Dyes Removal from Wastewater: Recent Review," *Management of Environmental Quality: An International Journal*, vol. 33, no. 2, pp. 451–477, 2022.

[6] A. Srivastava, R. M. Rani, D. S. Patle, and S. Kumar, "Emerging bioremediation technologies for the treatment of textile wastewater containing synthetic dyes: a comprehensive review," *Journal of Chemical Technology & Biotechnology*, vol. 97, no. 1, pp. 26–41, 2022.

[7] H. Chen, X. Wang, J. Li, and X. Wang, "Cotton derived carbonaceous aerogels for the efficient removal of organic pollutants and heavy metal ions," *Journal of Materials Chemistry A*, vol. 3, no. 11, pp. 6073–6081, 2015.

[8] M. Mariana, A. K. HPS, E. B. Yahya et al., "Recent trends and future prospects of nanostructured aerogels in water treatment applications," *Journal of Water Process Engineering*, vol. 45, p. 102481, 2022.

[9] A. Demirbas, "Agricultural based activated carbons for the removal of dyes from aqueous solutions: a review," *Journal of Hazardous Materials*, vol. 167, no. 1-3, pp. 1–9, 2009.

[10] S. B. Haderlein, K. W. Weissmahr, and R. P. Schwarzenbach, "Specific adsorption of nitroaromatic explosives and pesticides to clay minerals," *Environmental Science & Technology*, vol. 30, no. 2, pp. 612–622, 1996.

[11] S. Wang and Y. Peng, "Natural zeolites as effective adsorbents in water and wastewater treatment," *Chemical Engineering Journal*, vol. 156, no. 1, pp. 11–24, 2010.

[12] D. Vishnu, B. Dhandapani, S. Authilingam, and S. V. Sivakumar, "A comprehensive review of effective adsorbents used for the removal of dyes from wastewater," *Current Analytical Chemistry*, vol. 18, no. 3, pp. 255–268, 2022.

[13] A. K. Al-Buriahi, A. A. Al-Gheethi, P. S. Kumar et al., "Elimination of rhodamine B from textile wastewater using nanoparticle photocatalysts: a review for sustainable approaches," *Chemosphere*, vol. 287, p. 132162, 2022.

[14] M. Perwez, H. Fatima, M. Arshad, V. Meena, and B. Ahmad, "Magnetic iron oxide nanosorbents effective in dye removal," *International journal of Environmental Science and Technology*, 2022.

[15] B. Das, B. Das, N. S. Das, S. Sarkar, and K. K. Chattopadhyay, "Tailored mesoporous nanocrystalline Ga_2O_3 for dye-selective photocatalytic degradation," *Microporous and Mesoporous Materials*, vol. 288, p. 109600, 2019.

[16] Y. Wu, X. Du, Y. Kou, Y. Wang, and F. Teng, "Mesoporous SiO2 nanostructure: light-induced adsorption enhancement and its application in photocatalytic degradation of organic dye," *Ceramics International*, vol. 45, no. 18, pp. 24594–24600, 2019.

[17] H. Chaker, N. Ameur, K. Saidi-Bendahou, M. Djennas, and S. Fourmentin, "Modeling and Box-Behnken design optimization of photocatalytic parameters for efficient removal of dye by lanthanum-doped mesoporous TiO_2," *Journal of Environmental Chemical Engineering*, vol. 9, no. 1, p. 104584, 2021.

[18] Z. Yan, G. Li, L. Mu, and S. Tao, "Pyridine-functionalized mesoporous silica as an efficient adsorbent for the removal of acid dyestuffs," *Journal of Materials Chemistry*, vol. 16, no. 18, pp. 1717–1725, 2006.

[19] M. Anbia and S. Salehi, "Removal of acid dyes from aqueous media by adsorption onto amino- functionalized nanoporous silica SBA-3," *Dyes and Pigments*, vol. 94, no. 1, pp. 1–9, 2012.

[20] Y. Wu, M. Zhang, H. Zhao, S. Yang, and A. Arkin, "Functionalized mesoporous silica material and anionic dye adsorption: MCM-41 incorporated with amine groups for competitive adsorption of Acid Fuchsine and Acid Orange II," *RSC Advances*, vol. 4, no. 106, pp. 61256–61267, 2014.

[21] L. Adlnasab, M. Shabanian, M. Ezoddin, and A. Maghsodi, "Amine rich functionalized mesoporous silica for the effective removal of alizarin yellow and phenol red dyes from waste waters based on response surface methodology," *Materials Science and Engineering: B*, vol. 226, pp. 188–198, 2017.

[22] S. Shariati, A. Chinevari, and M. Ghorbani, "Simultaneous removal of four dye pollutants in mixture using amine functionalized Kit-6 silica mesoporous magnetic nanocomposite," *SILICON*, vol. 12, no. 8, pp. 1865–1878, 2020.

[23] J. R. Deka, Y.-H. Lin, and H.-M. Kao, "Ordered cubic mesoporous silica KIT-5 functionalized with carboxylic acid groups for dye removal," *RSC Advances*, vol. 4, no. 90, pp. 49061–49069, 2014.

[24] A. Feinle, F. Leichtfried, S. Straßer, and N. Hüsing, "Carboxylic acid-functionalized porous silica particles by a co-condensation approach," *Journal of Sol-Gel Science and Technology*, vol. 81, no. 1, pp. 138–146, 2017.

[25] J.-F. Lambert, "Adsorption and polymerization of amino acids on mineral surfaces: a review," *Origins of Life and Evolution of Biospheres*, vol. 38, no. 3, pp. 211–242, 2008.

[26] J. E. Rosen and F. X. Gu, "Surface functionalization of silica nanoparticles with cysteine: a low-fouling zwitterionic surface," *Langmuir*, vol. 27, no. 17, pp. 10507–10513, 2011.

[27] A. M. Beagan, "Investigating Methylene Blue removal from aqueous solution by cysteine-functionalized mesoporous silica," *Journal of Chemistry*, vol. 2021, Article ID 8839864, 12 pages, 2021.

[28] A. M. Alswieleh, "Remediation of cationic and anionic dyes from water by histidine modified mesoporous silica," *International Journal of Environmental Analytical Chemistry*, pp. 1–13, 2021.

[29] A. M. Alswieleh, "Cysteine-and glycine-functionalized mesoporous silica as adsorbents for removal of paracetamol from aqueous solution," *International Journal of Environmental Analytical Chemistry*, pp. 1–12, 2021.

[30] A. M. Alswieleh, H. Y. Albahar, A. M. Alfawaz et al., "Evaluation of the adsorption efficiency of glycine-, iminodiacetic acid-, and amino propyl-functionalized silica nanoparticles for the removal of potentially toxic elements from contaminated water solution," *Journal of Nanomaterials*, vol. 2021, Article ID 6664252, 12 pages, 2021.

[31] A. M. Alswieleh, M. M. Alshahrani, K. E. Alzahrani et al., "Surface modification of pH-responsive poly (2-(tert-butylamino) ethyl methacrylate) brushes grafted on mesoporous silica nanoparticles," *Designed Monomers and Polymers*, vol. 22, no. 1, pp. 226–235, 2019.

[32] A. M. Alswieleh, A. M. Beagan, B. M. Alsheheri, K. M. Alotaibi, M. D. Alharthi, and M. S. Almeataq, "Hybrid mesoporous silica nanoparticles grafted with 2-(tert-butylamino) ethyl methacrylate-b-poly (ethylene glycol) methyl ether methacrylate diblock brushes as drug nanocarrier," *Molecules*, vol. 25, no. 1, p. 195, 2020.

[33] C. Samart, S. Karnjanakom, C. Chaiya, P. Reubroycharoen, R. Sawangkeaw, and M. Charoenpanich, "Statistical optimization of biodiesel production from para rubber seed oil by SO_3H-MCM-41 catalyst," *Arabian Journal of Chemistry*, vol. 12, no. 8, pp. 2028–2036, 2019.

[34] K. M. Alotaibi, A. A. Almethen, A. M. Beagan et al., "Quaternization of poly (2-diethyl aminoethyl methacrylate) brush-grafted magnetic mesoporous nanoparticles using 2-Iodoethanol for removing anionic dyes," *Applied Sciences*, vol. 11, no. 21, p. 10451, 2021.

[35] K. M. Alotaibi, "Mesoporous silica nanoparticles modified with stimuli-responsive polymer brush as an efficient adsorbent for chlorophenoxy herbicides removal from contaminated water," *International Journal of Environmental Analytical Chemistry*, pp. 1–14, 2021.

[36] L. Hu, Z. Yang, Y. Wang et al., "Facile preparation of water-soluble hyperbranched polyamine functionalized multiwalled carbon nanotubes for high-efficiency organic dye removal from aqueous solution," *Scientific Reports*, vol. 7, no. 1, pp. 1–13, 2017.

[37] S. Ge, W. Geng, X. He et al., "Effect of framework structure, pore size and surface modification on the adsorption performance of methylene blue and Cu^{2+} in mesoporous silica," *Colloids and Surfaces A: Physicochemical and Engineering Aspects*, vol. 539, pp. 154–162, 2018.

[38] A. Ebadi and A. A. Rafati, "Preparation of silica mesoporous nanoparticles functionalized with β -cyclodextrin and its application for methylene blue removal," *Journal of Molecular Liquids*, vol. 209, pp. 239–245, 2015.

[39] Z. Jiaqi, D. Yimin, L. Danyang, W. Shengyun, Z. Liling, and Z. Yi, "Synthesis of carboxyl-functionalized magnetic nanoparticle for the removal of methylene blue," *Colloids and Surfaces A: Physicochemical and Engineering Aspects*, vol. 572, pp. 58–66, 2019.

[40] Y. Li, Y. Zhou, W. Nie, L. Song, and P. Chen, "Highly efficient methylene blue dyes removal from aqueous systems by chitosan coated magnetic mesoporous silica nanoparticles," *Journal of Porous Materials*, vol. 22, no. 5, pp. 1383–1392, 2015.